

B. Maqsood

# Cloudier Skies

Marine Cloud Brightening: How Sea Salt Aerosol Properties Relate to the Brightening of Stratocumulus Clouds



# Cloudier Skies

## Marine Cloud Brightening: How Sea Salt Aerosol Properties Relate to the Brightening of Stratocumulus Clouds

By

**B. Maqsood**

in partial fulfilment of the requirements for the degree of

### **Bachelor of Science** in Civil Engineering

at the Delft University of Technology  
to be presented on Monday October 26, 2020

Supervisor: Dr.sc. F. Glassmeier  
Thesis committee: Dr. R.E.M. Riva, Delft University of Technology  
Dr.sc. F. Glassmeier, Delft University of Technology

Student number: 4375009



# Preface

Hereby, I present my thesis report of the Bachelor's Final Project which is included in the curriculum of the BSc programme Civil Engineering at the Delft University of Technology. By using a numerical model, I have determined how physical properties of sea salt aerosol relate to the albedo when a cloud is brightened through marine cloud brightening.

I would like to thank my supervisor Dr.sc. Franziska Glassmeier for introducing this topic and the numerical model to me, for her guidance during the project and for the provided feedback which helped me a lot. Thanks to her, I am more interested in this field of engineering.

Also, I want to thank Dr. Riccardo Riva for his interest in my thesis and his feedback. I appreciate his willingness to be part of the thesis committee.

I hope you will enjoy reading my thesis report.

Bilal Maqsood  
Rotterdam, October 2020



# Abstract

Over the period 1901-2012, the average global sea surface temperature has increased by 0.89 °C due to climate change and it is expected to increase consistent with global warming. As a consequence, marine ecosystems have become more susceptible to change in species and ocean chemistry. Due to the increase in sea surface temperature, the ocean pH has decreased in all regions. The main driver for this development is the uptake of approximately 30% of anthropogenic carbon dioxide (CO<sub>2</sub>) by oceans (IPCC, 2014). In a warming ocean, populations of warm-water species grow and populations of cold-water species decline. Furthermore, declines in coral growth are observed (Poloczanska et al., 2016).

Marine cloud brightening is a proposed way to counteract climate change. This geo-engineering technique brightens clouds by spraying aerosols in the air which act as cloud condensation nuclei in order to form cloud droplets. As a result, the albedo of the brightened cloud increases and more sunlight is reflected, reducing the global mean temperature (Latham et al., 2012). Although it is a potential way to counteract climate change, marine cloud brightening has never been applied on a large scale. Also, little is known about its feasibility.

We determined how physical properties of sea salt aerosols, specifically the aerosol mean geometric radius, the aerosol number concentration and the modal standard deviation of the initial aerosol spectrum, relate to the albedo of the brightened cloud using a numerical cloud parcel model with input parameters (Glassmeier et al., 2020). For six different values of the initial aerosol mean geometric radius, the initial aerosol number concentration and the modal standard deviation of the initial aerosol spectrum, i.e. the variability in aerosol radius, three output variables were generated in time and height. These output variables were the mean radius of cloud droplets, the cloud droplet number and the relative supersaturation. The differences caused by varying the input parameters were interpreted for the output variables. Also, we generated the albedo for the six different values of each input parameter mentioned.

The cloud droplet number depends on the aerosol number concentration. The higher the number, the more cloud droplets are formed. The cloud albedo does not depend on the initial aerosol mean geometric radius. The moment of activation depends on the initial aerosol mean geometric radius and the initial aerosol number concentration. The growth of the cloud droplets is mainly driven by condensation when variability in aerosol radius is small. The higher the initial aerosol number concentration, the higher the albedo of the brightened cloud. When the variability in radius is bigger, collision-coalescence occurs as the spectrum of cloud droplets consists of bigger radii which tend to collide and coalesce. This leads to bigger and heavier droplets which precipitate due to an increased mass, resulting in a decrease in cloud droplet number and a decrease in cloud albedo.

To conclude, three relations between physical properties of sea salt aerosol and the cloud albedo were found. First, the aerosol mean geometric radius at start does not affect the cloud albedo. Secondly, we found that the higher the aerosol number concentration, the higher the cloud albedo. Furthermore, a higher modal standard deviation of the initial aerosol spectrum leads to a lower cloud albedo.

We recommend further research on other types of aerosols, like organic matter and algae, and the effect of external forcing, like wind, on cloud brightening.



# Table of Contents

Preface.....	V
Abstract.....	VII
1 Introduction.....	1
2 Methodology.....	3
2.1 Cloud parcel model and input parameters.....	3
2.2 Simulations and microphysical variables.....	4
3 Results.....	6
3.1 Influence of varying the aerosol mean geometric radius.....	6
3.2 Influence of varying the aerosol number concentration.....	9
3.3 Influence of varying the modal standard deviation of the initial aerosol spectrum.....	11
3.4 Spectra of cloud droplet size for three different modal standard deviations.....	13
4 Discussion.....	15
5 Conclusions and Recommendations.....	16
A Python code for plots aerosol mean geometric radius at start.....	18
B Python code for plots aerosol number concentration at start.....	20
C Python code for plots modal standard deviation of initial aerosol spectrum.....	22
References.....	24



# Introduction

Since 1988, the Intergovernmental Panel on Climate Change (IPCC) is responsible for assessments of the changing climate. Consisting of 195 member countries, the IPCC considers different climate scenarios and reviews research on consequences of a changing climate such as the change in global average surface temperature and the global mean sea level rise. According to the IPCC (2017), it “provides regular assessments of the scientific basis of climate change, its impacts and future risks, and options for adaptation and mitigation”. These regular assessments are presented in assessment reports. In its latest report, it is projected that the global average surface temperature will likely increase by 1.5 °C to 2.0 °C (IPCC, 2014). As a consequence, the global mean sea level is projected to rise 0.5 to 1.4 meters with respect to 1990 (Rahmstorf, 2007). These changes will have significant impact on weather around the world. Frequency and intensity of precipitation will alter. The number of cold days will decrease, and the number of warm days will increase. Extreme weather will occur more often, leading to social-economical damage.

Consistent with the global average surface temperature, the average global sea surface temperature is increasing as well. Over the period 1901-2012, the change was an increase of 0.89 °C as oceans have taken approximately 30% of anthropogenic carbon dioxide (CO<sub>2</sub>) (IPCC, 2014). This has resulted in a decreased ocean pH and an altered ocean chemistry in all ocean regions with consequences for marine organisms. In a warming ocean, populations of warm-water species will grow, while populations of cold-water species are expected to decline. Poloczanska et al. (2016) indicate that 52% of 346 observed warm species shows an increase. The same percentage of 293 observed cold species shows decline with disturbed ecosystems as consequence (p. 10). Furthermore, declines in calcification and growth rates are observed in skeletons of corals (Poloczanska et al., 2016).

To combat the warming of the planet, marine cloud brightening has been suggested. Marine cloud brightening is a proposed geo-engineering technique aiming to brighten clouds by increasing the flux of cloud condensation nuclei in the form of sea salt aerosols (Horowitz et al., 2020). By creating a flux of aerosols, stratocumulus clouds above oceans will be seeded with an enormous amount of sea salt aerosols with sub-micrometer radii. By doing so, the amount of cloud droplets might significantly increase, resulting in an increased albedo (Latham et al., 2012). An increased albedo will make the brightened cloud reflect more sunlight and decrease the global mean temperature. Several designs of marine cloud brightening have been suggested. One of those consists of an unmanned vessel, wind-powered, featuring a spray mechanism. This vessel would spray sea salt aerosols with a certain radius (Gadian, 2009). An impression of this design is depicted in figure 1.1.

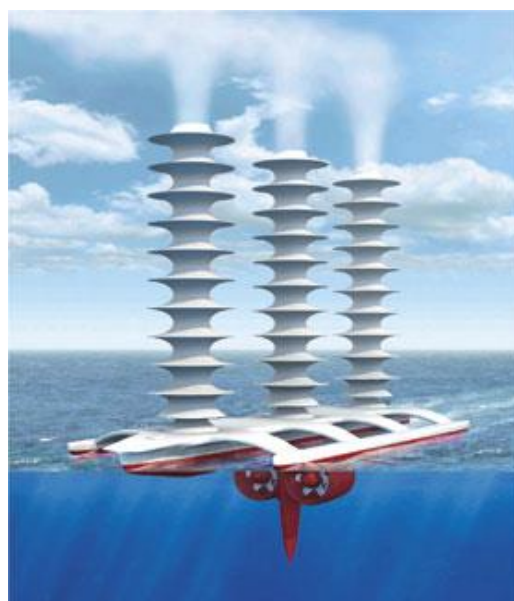


Figure 1.1 Impression of a marine cloud brightening vessel (Gadian, 2009)

In this thesis report, we use an adiabatic cloud parcel model (Glassmeier et al., 2020) which describes the microphysical processes occurring when a cloud is brightened. Basically, a parcel ascends with a constant updraft speed and contains a certain number of cloud condensation nuclei. While ascending to a cloud top height, the model describes cloud microphysical processes occurring in the parcel due to the presence of cloud condensation nuclei, such as cloud droplet and rain formation after reaching the lifting condensation level. This numerical model uses budget equations depending on a source and sink. Furthermore, the model uses physical properties of the used aerosols as input and generates data about the process of cloud brightening. Figure 1.2 illustrates the concept of the cloud parcel model.

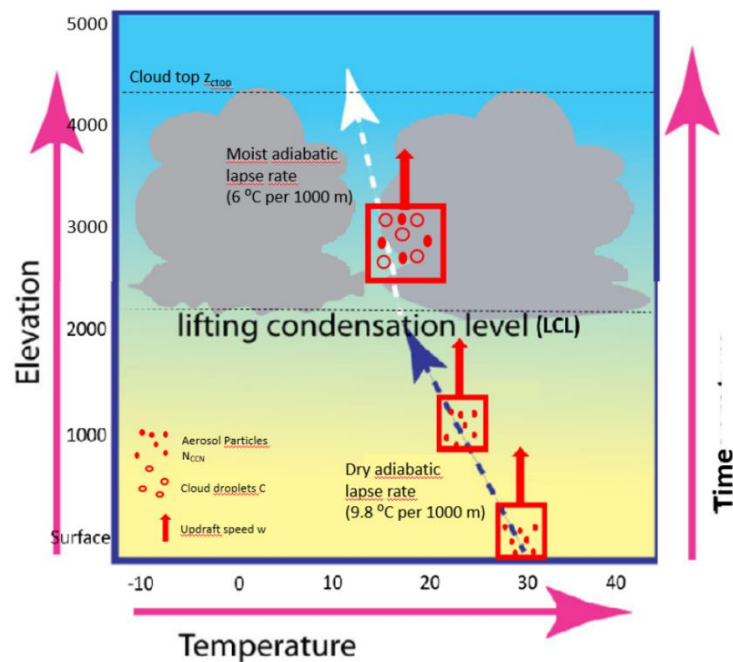


Figure 1.2 The concept of the cloud parcel model (Glassmeier et al., 2020)

The aim of this thesis is to derive a relation between the sea salt aerosol properties and the extent of brightening in order to optimize the engineering behind marine cloud brightening. Thus, the research question is:

*How do physical properties of sea salt aerosol relate to the albedo of the brightened cloud?*

Next to obtaining an answer to this question, we also aim to interpret what processes determine the albedo of a brightened cloud. In Chapter 2, the methodology is explained. Also, the parameters for the simulations are determined. In Chapter 3, the results are presented by plots of output variables in time and height and by spectra, and an interpretation is given. Chapter 4 discusses limitations of the research. In Chapter 5, the research question is answered based on the results and recommendations are given.

# Methodology

## 2.1 Cloud parcel model and input parameters

To find a relation between the physical properties of sea salt aerosols and the cloud albedo, we carried out simulations using a numerical model, written in Fortran. This numerical model is based on the adiabatic cloud parcel model as described in the technical report “*Introduction to the adiabatic cloud parcel model*” (Glassmeier et al., 2020) and enables us to study cloud microphysics. To run the model, we used it as an ipython notebook in Google Colaboratory.

The cloud parcel model is based on equations which describe the microphysical processes in the parcel. These equations consist of a sink and a source component. Equation (1) describes the change in relative supersaturation over time.  $Q_0$  relates to diffusion of vapor and latent heat.  $Q_1$  relates to the relative humidity. Equation (2) shows the change in radius over time. The change in total radius depends on change in radius due to condensation and due to collision-coalescence. Furthermore, Equation (3) represents the change in cloud droplet number over time depending on activation of aerosols and collision-coalescence. Activation is the moment when an aerosol forms a cloud droplet which starts to grow due to condensation. Larger cloud droplets collide and coalesce, resulting in a decrease of the cloud droplet number (Glassmeier et al., 2020).

$$\frac{dS}{dt} = Q_1 * w - Q_0 * S * N * \langle r \rangle \quad (1)$$

$$\frac{dr}{dt} = \left. \frac{dr}{dt} \right|_{cond} + \left. \frac{dr}{dt} \right|_{cc} \quad (2)$$

$$\frac{dN}{dt} = \left. \frac{dN}{dt} \right|_{act} - \left. \frac{dN}{dt} \right|_{cc} \quad (3)$$

The change in radius due to condensation, which is the first term of Equation (2), is represented by Equation (4).  $F_k$  represents the latent heat release and  $F_d$  represents diffusion of water vapor towards growing droplets. Equation (5) shows that the relative supersaturation is dependent on the droplet radius (Glassmeier et al., 2020).

$$\left. \frac{dr}{dt} \right|_{cond} = \frac{1}{F_k + F_d} * \frac{1}{r} * S_r(r) \quad (4)$$

$$S = \frac{a}{r} - \frac{b}{r^3} \quad (5)$$

The model uses input parameters related to the physical properties of the sea salt aerosols. These are the density, molecular weight and the dissociation factor of the aerosol and are used in equations which the model is based on. We determined the density of sea salt to be 2170 kg/m<sup>3</sup> according to annual global average values of Guelle et al. (p. 27520, 2001). The molecular weight of sea salt, sodium chloride, is 0.0585 kg/mol and the dissociation factor is 2 (National Library of Medicine, 2020). These values are given in table 2.1. For all simulations, these values did not change. Furthermore, the aerosol number concentration at start of the simulation are relevant alongside the initial aerosol mean geometric radius and the modal standard deviation of initial aerosol spectrum.

Table 2.1 Physical properties of sea salt

Physical property	Value
Density	2170 kg/m <sup>3</sup> (Guelle et al., 2001)
Dissociation factor	2
Molecular weight	0.0585 kg/mol (National Library of Medicine, 2020)

Next to the physical properties, the model requires an updraft speed, an initial height and the height of the cloud top. We chose the updraft speed to be 0.3 m/s in accordance with sensitivity studies performed by Connolly et al. (2014). The height of the cloud top is 1500 m, which is characteristic for stratocumulus clouds (MetOffice, 2020). The initial height is 5 meters. This height represents the length of the spraying mechanism. According to the model, this is the starting height of the parcel with respect to the ocean surface. These values are given in table 2.2.

Table 2.2 Parameters for the simulations

Parameter	Value
Updraft speed	0.3 m/s (Connolly et al., 2014)
Height of cloud top	1500 m (Met Office, 2020)
Starting height	5 m

Based on these input parameters, we carried out the simulations. We chose the values given in table 2.1 and 2.2 to approach marine cloud brightening with sea salt aerosols. With these parameters the model provided output data discussed in Section 2.2.

## 2.2 Simulations and microphysical variables

As output, the numerical model generates data consisting of 28 variables describing cloud microphysics within the cloud parcel in time and height. We used the following three variables as their change over time is described by the parcel model:

- mean radius of cloud droplets
- cloud droplet number/liquid number mixing ratio
- relative supersaturation

For each of these variables, we ran simulations at six different values for three different parameters. These parameters are the aerosol mean geometric radius at start, the aerosol number concentration at start and the modal standard deviation of the initial aerosol spectrum. The six different values of each of these parameters for the simulations are given in table 2.3.

Note that we did not keep these parameters constant, unlike the other parameters. By carrying out simulations for 6 different values of each parameter mentioned above, we extracted data for the mean radius of cloud droplets, the cloud droplet number and the relative supersaturation. With this data, we plotted the development of these three variables in time and height using Python in Jupyter Notebook. Besides, we also computed the albedo for all values of each parameter varied. Furthermore, we made spectra of cloud droplet sizes for three different modal standard deviations:  $\sigma = 1.0$ ,  $\sigma = 1.2$  and  $\sigma = 2.0$ , in order to describe what the influence of variability in aerosol radius is.

When one of the three parameters varied during the simulations, we kept the other two constant. In table 2.3, the values of the parameters kept constant are given.

Table 2.3 Six different values for the varied parameters

Parameter	Values for simulations
Aerosol mean geometric radius at start	$r_{mg} = 0.015 \mu\text{m}$ , $r_{mg} = 0.020 \mu\text{m}$ , $r_{mg} = 0.045 \mu\text{m}$ , $r_{mg} = 0.085 \mu\text{m}$ , $r_{mg} = 0.170 \mu\text{m}$ , $r_{mg} = 0.200 \mu\text{m}$ ,
Aerosol number concentration at start	$N = 5 \times 10^6/\text{m}^3$ , $N = 10 \times 10^6/\text{m}^3$ $N = 15 \times 10^6/\text{m}^3$ , $N = 20 \times 10^6/\text{m}^3$ $N = 25 \times 10^6/\text{m}^3$ , $N = 30 \times 10^6/\text{m}^3$
Modal standard deviation of initial aerosol spectrum	$\sigma = 1.0$ , $\sigma = 1.2$ , $\sigma = 1.4$ $\sigma = 1.6$ , $\sigma = 1.8$ , $\sigma = 2.0$
When aerosol mean geometric radius at start varied	$N = 1 \times 10^7/\text{m}^3$ , $\sigma = 1.0$
When aerosol number concentration at start varied	$r_{mg} = 0.085 \mu\text{m}$ , $\sigma = 1.0$
When modal standard deviation varied	$r_{mg} = 0.085 \mu\text{m}$ , $N = 1 \times 10^7/\text{m}^3$

# 3 Results

By using the adiabatic cloud parcel, we plotted the mean radius of cloud droplets, the cloud droplet number and the relative supersaturation for six different values of the aerosol mean geometric radius at start, the initial aerosol number concentration and the modal standard deviation of the initial aerosol spectrum. The plots show the development of these variables in time and height. In this chapter, we interpret these results with equations given in Section 2.1. Furthermore, we consider droplet size spectra for three different modal standard deviation. These will be interpreted as well.

## 3.1 Influence of varying the aerosol mean geometric radius

Varying the aerosol mean geometric radius at start leads to a different development of the mean radius of the cloud droplets in time and height. As can be seen in figure 3.1a, the activation occurs after approximately 2000 seconds and at a height of 600 meters. But for a changing initial aerosol mean geometric radius, it takes longer for a smaller radius until activation occurs. Nevertheless, the mean radius of cloud droplets develops in the same manner for all initial aerosol mean geometric radius after approximately 2200 seconds and when the mean radius of cloud droplets equals approximately 18  $\mu\text{m}$ .

The difference in moment of activation can also be seen in figure 3.1b. The cloud droplet number is equal for all initial aerosol mean radii after activation, namely approximately  $8.5 \times 10^6$  droplets/kg. After activation the cloud droplet number stays equal.

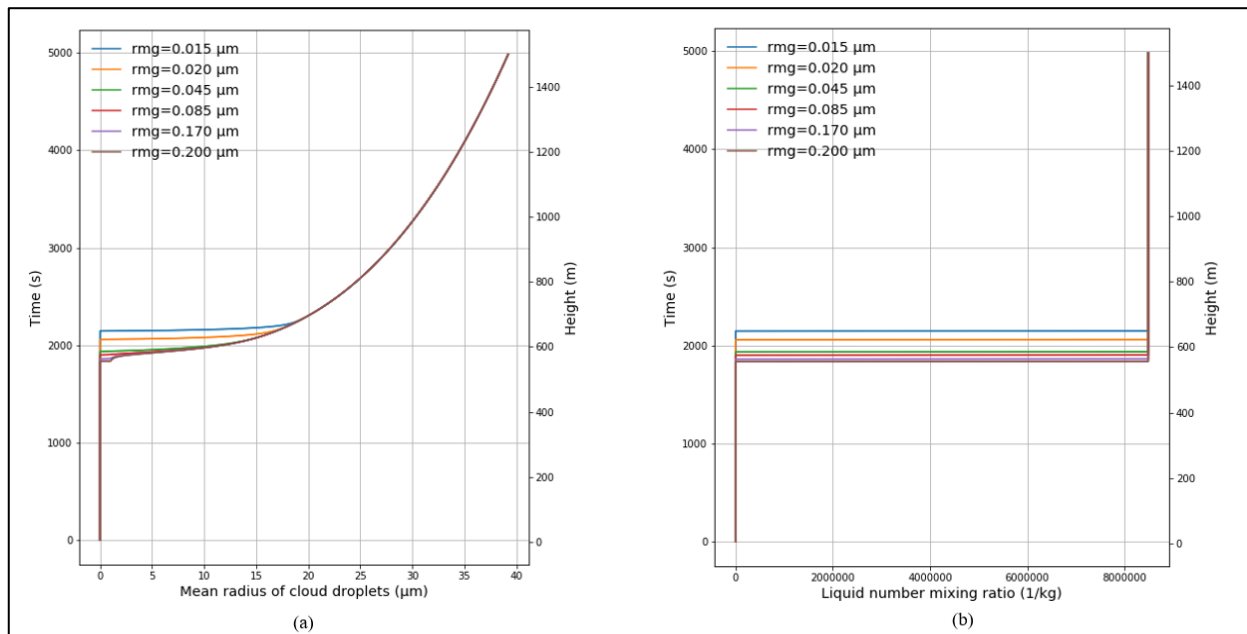


Figure 3.1 Change in mean radius of cloud droplets (a) and cloud droplet number (b) for six different aerosol mean geometric radii

Figure 3.2a shows the change of relative supersaturation in time and height for the different values of aerosol mean geometric radius at start. For all radii, the relative supersaturation increases at a constant rate. When activation occurs, the relative supersaturation decreases to slightly above 0 for all initial aerosol mean geometric radii. This 'drop' in relative supersaturations happens at the height and moment of activation. A delay in activation for smaller radii can be seen in this figure as well.

In figure 3.2b, it can be seen that the smaller the aerosol mean geometric radius at start, the higher the relative supersaturation at activation.

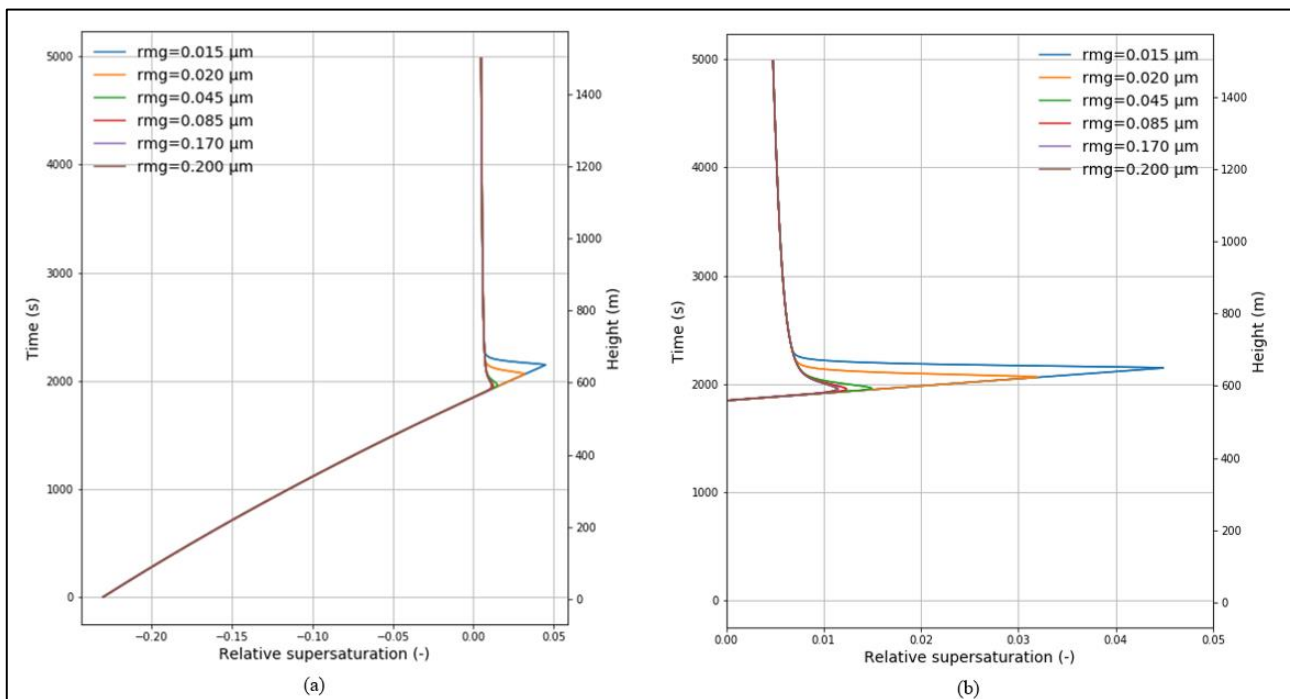


Figure 3.2 Change in relative supersaturation for six different aerosol mean geometric radii (a). (b) zooms into (a)

Change in albedo by varying the aerosol mean geometric radius at start is depicted in figure 3.3. It can be seen that the albedo mainly stays constant. For all chosen aerosol mean geometric radii, the albedo equals 0.86.

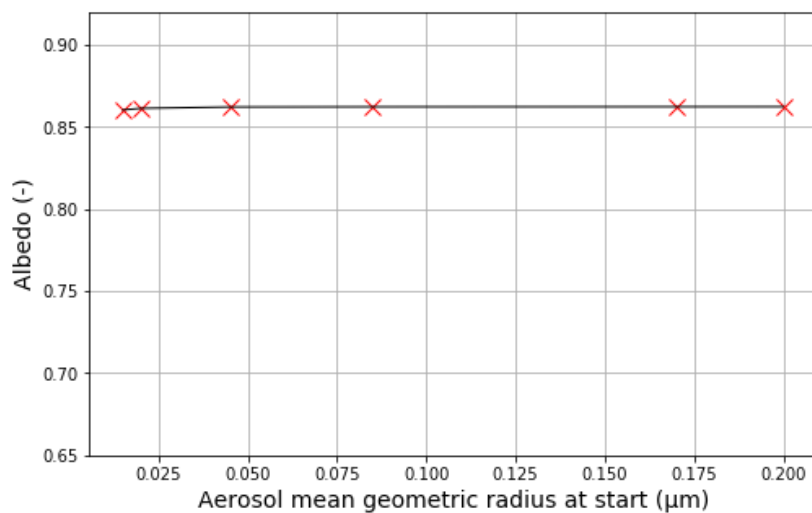


Figure 3.3 Change in albedo at changing aerosol mean geometric radius at start

The albedo does not seem to be depending on the mean geometric radius of the aerosol which is used. The underlying reason for the albedo being constant is the equal value for the cloud droplet number for every aerosol mean geometric radius at start, as depicted in figure 3.1b. According to Boers and Mitchell (1994), the albedo depends on the mixing parameter  $\beta$ , cloud droplet number  $N$  and cloud thickness  $h$  as stated in Equation (6) (p. 231). In this Equation,  $\tau$  is the cloud optical depth and relates to the albedo.

$$\tau = C * (1 - \beta)^{\frac{2}{3}} * N^{\frac{1}{3}} * h^{\frac{5}{3}} \quad (6)$$

The equal growth of the mean radius of cloud droplets after approximately 2200 seconds, as shown in figure 3.1a, is explained by Equation (4). The increase in mean radius of the cloud droplet is mainly driven by condensation as the droplets are too small for collision-coalescence to occur. The change in radius of a cloud droplet depends on the radius itself. Right after activation, the change for smaller aerosols will be higher than the change for bigger aerosols. Consequently, a rapid growth will lead to a slower growth because of the rapid increase in droplet radius. This makes the mean radius of the cloud droplets grow equally from a certain point. Furthermore, the relative supersaturation becomes equal for all radii after activation as can be seen in figure 3.2b.

The relative supersaturation at activation increases with decreasing aerosol mean geometric radius. This can be explained by Equation (1). When activation happens, the relative supersaturation starts decreasing. This implies that the change in relative supersaturation over time becomes negative, so Equation (1) becomes negative. The increase before activation is determined by the first term of Equation (1) only, which appears to be positive and equal for all mean geometric radii. At activation, the second term also applies as Equation (1) needs to become 0. The second term depends on the cloud droplet number, the mean radius and the relative supersaturation itself. When the mean radius of the aerosols is too small to let Equation (1) become negative, the activation will be delayed until an increased value for the relative supersaturation making the second term larger than the first term. This explanation is consistent with Equation (5), the Köhler theory, which describes the activation of aerosols into clouds droplets and states that smaller aerosols require higher supersaturations for activation.

The reason why the cloud droplet number is equal for all initial aerosol radii is because the aerosol number concentration at start is equal.

### 3.2 Influence of varying the aerosol number concentration

When the aerosol number concentration at start varies, the mean radius of cloud droplets depends on the initial concentration. In figure 3.4a, it is depicted that the higher the initial aerosol number concentration, the lower the mean radius of the cloud droplets at a certain time and height. The figure also shows that the moment of activation is nearly equal for all initial aerosol concentrations. The activation seems to occur after approximately 1900 seconds at a height of approximately 590 meters.

In contrast to varying the aerosol mean geometric radius at start, different initial aerosol number concentrations lead to a different cloud droplet number. Figure 3.4b shows that the lower the aerosol number concentration at start, the lower the cloud droplet number after activation.

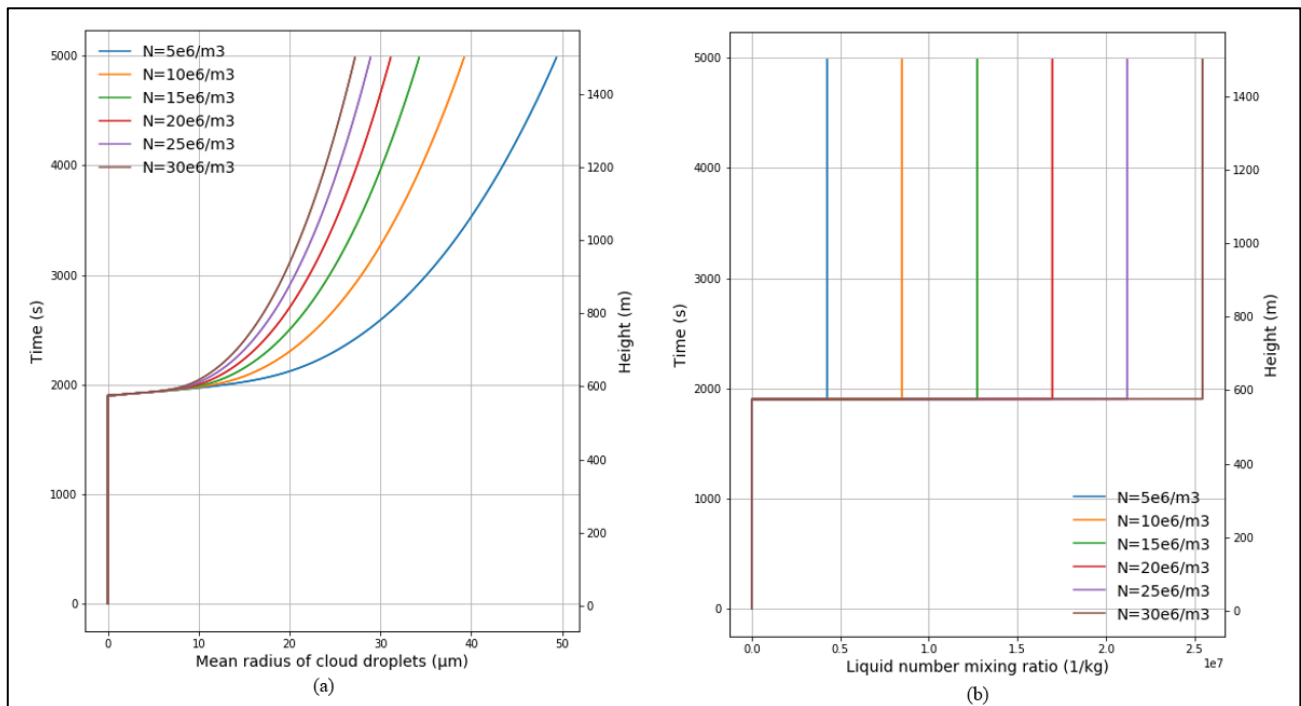


Figure 3.4 Change in mean radius of cloud droplets (a) and cloud droplet number (b) for six different aerosol number concentrations

Figure 3.5a depicts the change of relative supersaturation in time and height for the different aerosol number concentrations at start. In contrast to varying the aerosol mean geometric radius at start, the margin of difference is smaller. In figure 3.5b, it is depicted that the relative supersaturation at activation is higher when the initial aerosol number concentration is smaller. Furthermore, the relative supersaturation increases in the same rate. At activation, it decreases to slightly above 0.

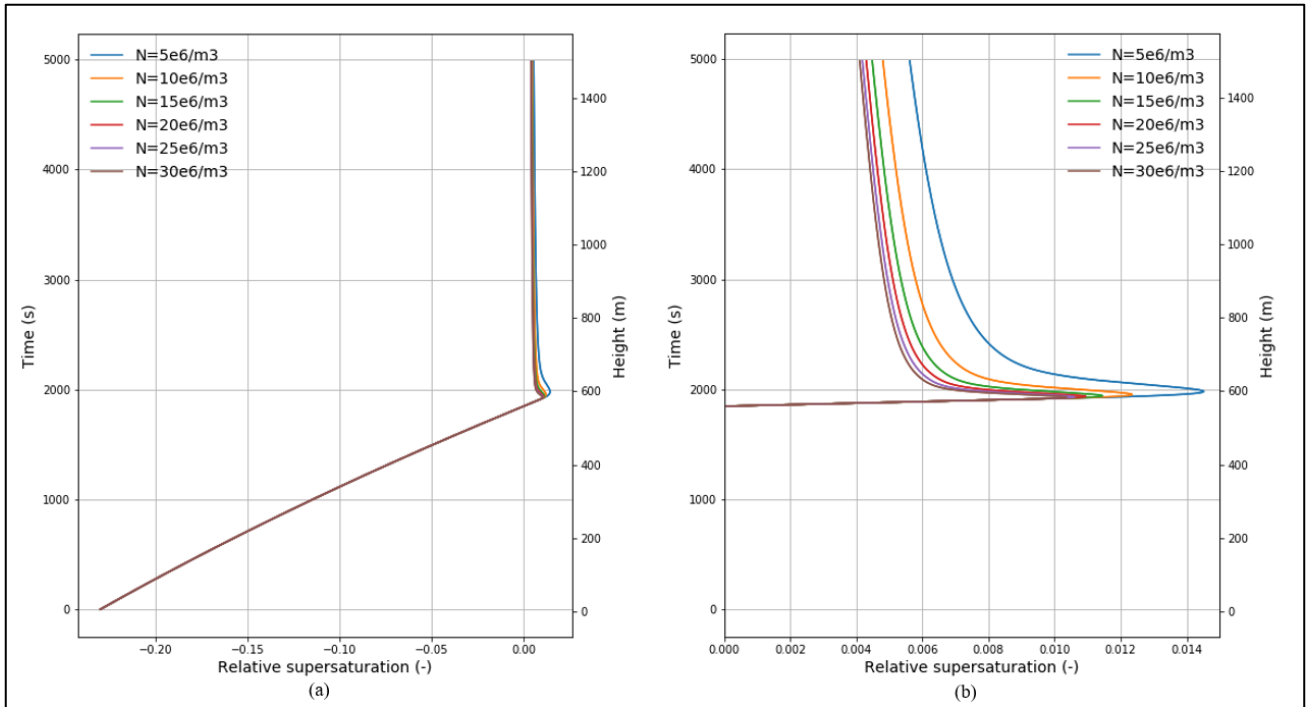


Figure 3.5 Change in relative supersaturation for six different aerosol number concentrations (a). (b) zooms into (a)

In figure 3.6, the albedo is plotted against the aerosol number concentration at start. The albedo increases with increasing initial concentration. With a concentration of  $5 \times 10^6/\text{m}^3$ , an albedo of approximately 0.83 is reached. A concentration of  $30 \times 10^6/\text{m}^3$  leads to an albedo of approximately 0.90.

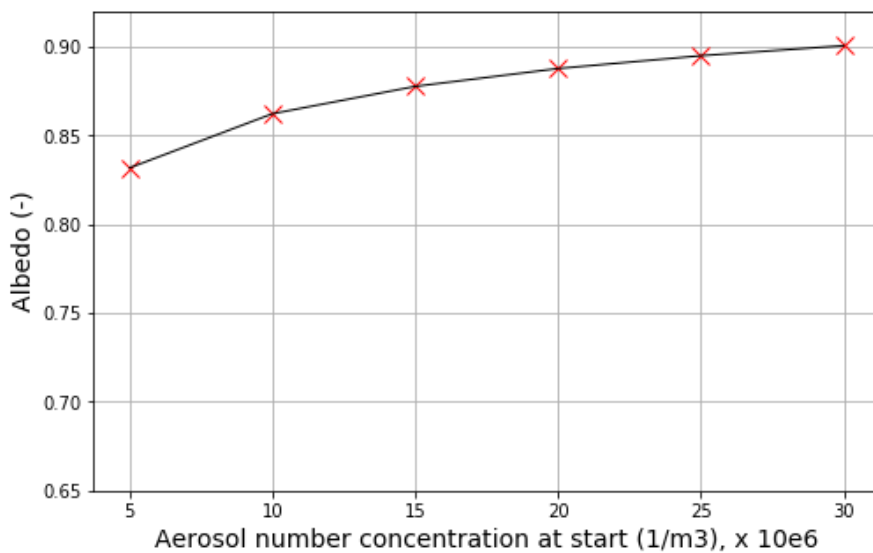


Figure 3.6 Change in albedo at changing aerosol number concentration at start

The increasing albedo at higher aerosol number concentrations at start is the result of an increased activation. A higher concentration of cloud droplets has a higher cloud droplet number as a higher number of aerosols activates. This means that the cloud is brighter and can reflect more sunlight.

Equation (1) explains why the relative supersaturation at activation is higher when the initial aerosol number concentration is smaller. This can be explained in a same way as for the aerosol mean geometric radius. The relative supersaturation slightly needs to increase in order for the equation to become negative.

As shown in figure 3.4a, the development of the mean radius of the cloud droplets depend on the aerosol number concentration at start. Because the droplets are too small to collide and coalesce, the increase in mean radius is mainly driven by condensation. To explain the difference caused by the aerosol number concentration at start, Equation (4) needs to be considered. This equation implies that the change in radius depends on the radius itself but also the relative supersaturation. As the relative supersaturation shows higher values for lower initial aerosol concentrations at start, the change in mean radius in time is scaled with a higher factor. This result in a faster increase in mean radius of the cloud droplets when using a lower concentration of aerosols.

### 3.3 Influence of varying the modal standard deviation of the initial aerosol spectrum

Figure 3.7a depicts how the mean radius of the cloud droplets depends on the modal standard deviation of the initial aerosol spectrum. As it can be seen, the cloud droplets become bigger when the modal standard deviation is higher than 1.0. Activation takes place after approximately 1900 seconds for all modal standard deviations. Due to a low cloud droplet number, the top of the graphs for modal standard deviations higher than 1 can statistically be seen as noise.

In figure 3.7b, the change of the cloud droplet number over time and height is shown. Contrary to figure 3.1b and 3.4b, the cloud droplet number does not stay constant after activation but decreases to 0 for all values of modal standard deviations except for  $\sigma$  equal to 1. Furthermore, aerosols belonging to initial spectra with values higher than 1 for the modal standard deviation activate earlier or even at the start before the activation after 1900 seconds.

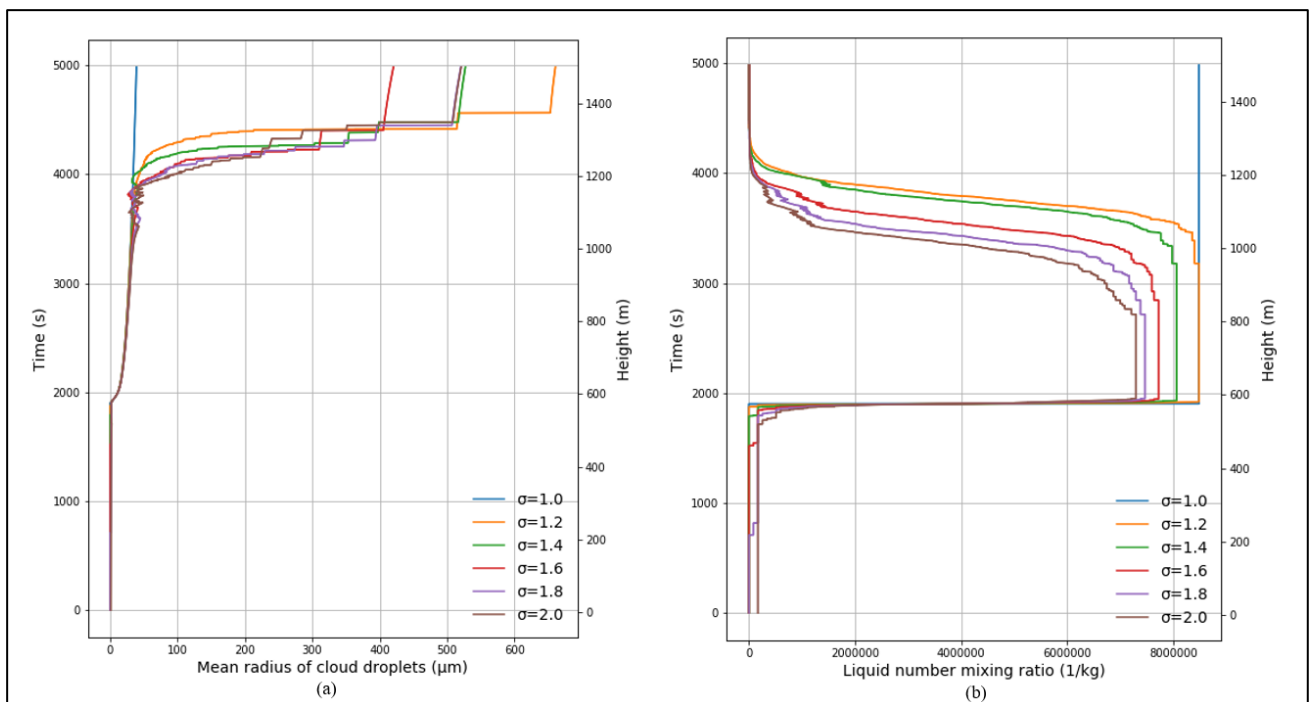


Figure 3.7 Change in mean radius of cloud droplets (a) and cloud droplet number (b) for six different initial aerosol spectra

How the relative supersaturation develops at different values for the modal standard deviation can be seen in figure 3.8. Varying the modal standard deviation does not seem to have any influence on the moment of activation.

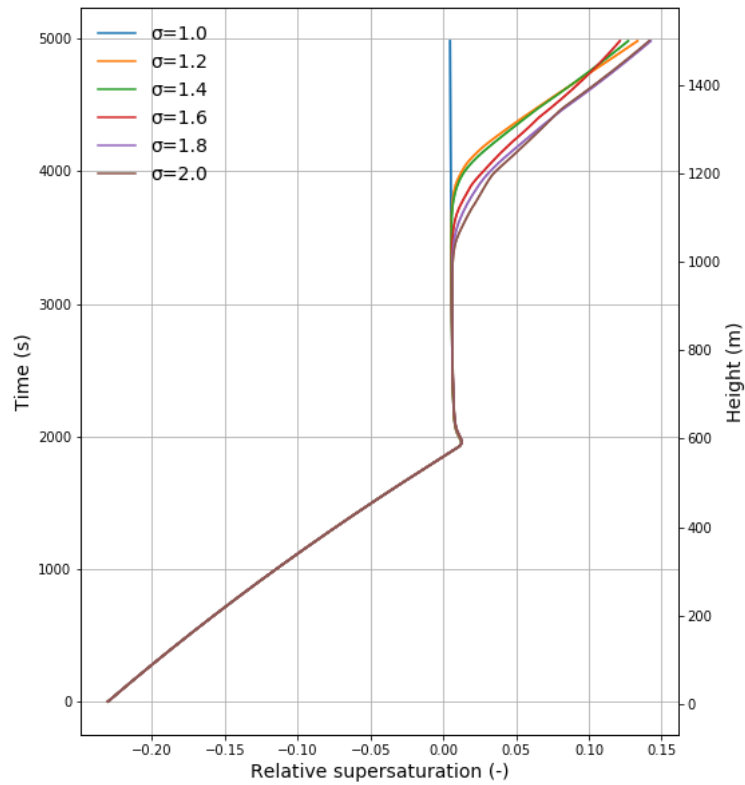


Figure 3.8 Change in relative supersaturation for six different initial aerosol spectra

The albedo decreases with increasing modal standard deviation of initial spectrum. At a modal standard deviation of 1.0, the albedo equals 0.86. At a modal standard deviation of 2.0, the albedo decreases to 0.69. This is depicted in figure 3.9.

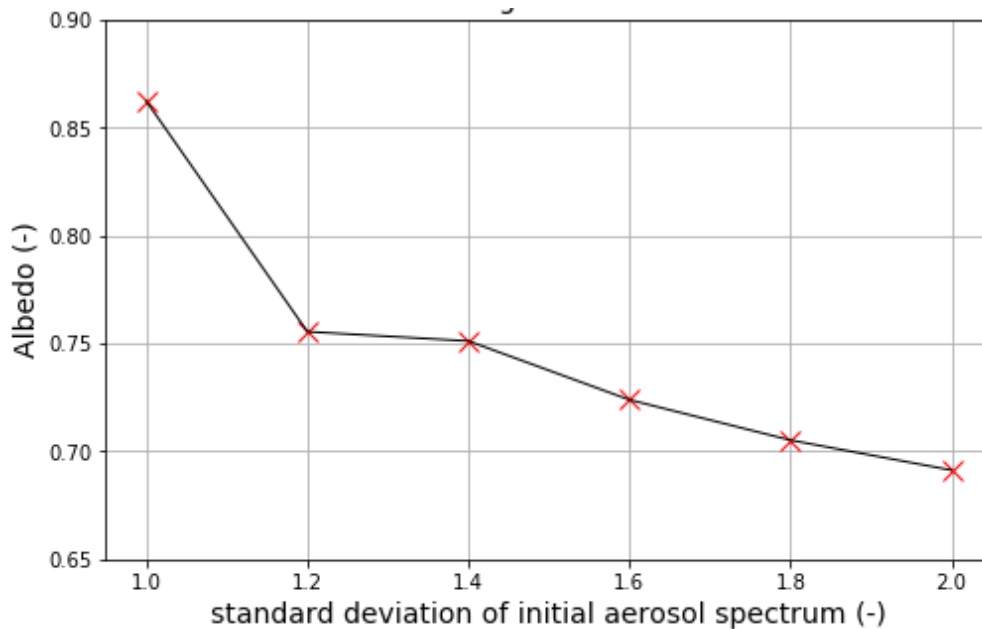


Figure 3.9 Change in albedo at changing initial aerosol spectrum

An initial aerosol spectrum with a high modal standard deviation leads to a low value for the albedo. This can be explained by the reduced amount of cloud droplets due to precipitation for modal standard deviations higher than 1.

For all modal standard deviations, the activation occurs at the same time and height, namely after approximately 2000 seconds. Initially, the mean radius of the cloud droplets increases in a similar rate for all modal standard deviations. But eventually, the mean radius increases faster for modal standard deviations higher than 1.0. This happens after approximately 4000 seconds due to occurrence of higher aerosol radii in higher numbers within the spectrum. These aerosols are able to activate earlier because of their size. As mentioned before, this activation occurs after approximately 1900 seconds. Furthermore, they tend to collide and coalesce with each other when they have increased in size. This collision-coalescence starts after approximately 4000 seconds and enables a reaction between the cloud droplets making them merge in a high pace ('cascade-effect'). This explains the spontaneous increase in mean radius of the cloud droplets.

Figure 3.7b shows early activations for  $\sigma = 1.6$  and  $\sigma = 1.8$ . For  $\sigma = 2.0$ , activation even starts immediately at  $t=0$ . These smaller activations occur due to aerosols with higher radii. These occur in higher numbers within the aerosol spectrum. The explanation for the different cloud droplet numbers due to activation at approximately 2000 seconds is the occurrence of aerosols with smaller radii in also high numbers at higher modal standard deviations. These hardly activate to form cloud droplets.

It is shown that the cloud droplet number decreases after staying constant. It eventually becomes 0 for all modal standard deviations higher than 1. This is due to the cloud droplets becoming heavy enough to theoretically precipitate. This occurs mainly due to collision-coalescence. This decrease in cloud droplet number explains the increase in relative supersaturation after approximately 3500 seconds for modal standard deviations higher than 1. The change over time becomes positive again as the cloud droplet number decreases and eventually becomes zero. This is in accordance with Equation (1).

### 3.4 Spectra of cloud droplet size for three different modal standard deviations

To visualize how many cloud droplets are formed and what radii they have, a spectrum of cloud droplet sizes can be used. This spectrum shows the evolution of the droplet number and size. In figures 3.10a and b, the spectra are given for an initial aerosol spectrum with a modal standard deviation of 1.0 and 2.0.

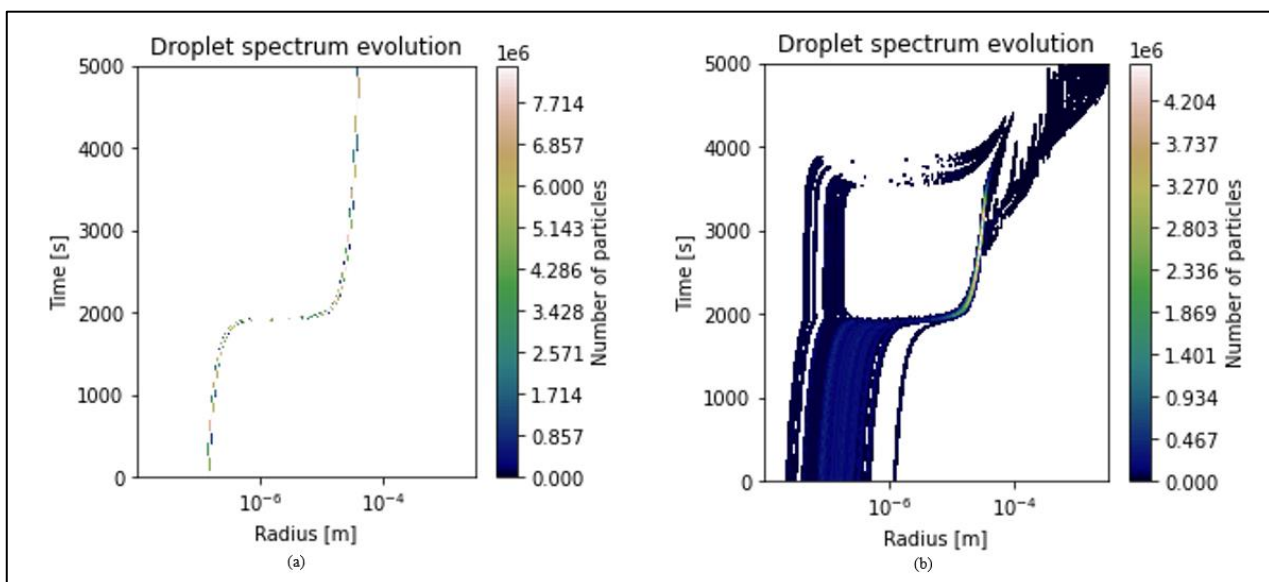


Figure 3.10 Spectra of cloud droplets for (a)  $\sigma=1.0$  and (b)  $\sigma=2.0$

Figure 3.10a shows the minimum variability in aerosol radius at start. Furthermore, the number of cloud droplets formed stays equal in time. After approximately 1900 seconds, the aerosols activate. This results in an increase of the radius. After activation, the radii increase very slightly due to condensation

For a modal standard deviation of 2.0, figure 3.10b shows a larger extent in variability. During activation, not all aerosols get activated. The smaller aerosols keep their initial radius. However, the bigger aerosols do activate and grow during condensation. A part collides and coalesces to precipitate eventually as depicted in the right top corner of figure 3.10b. The smaller aerosols eventually activate as well after approximately 4000 seconds. The same developments are depicted for  $\sigma=1.2$  in figure 3.11. But in this case the extent of variability is smaller, and all aerosols activate at the same time.

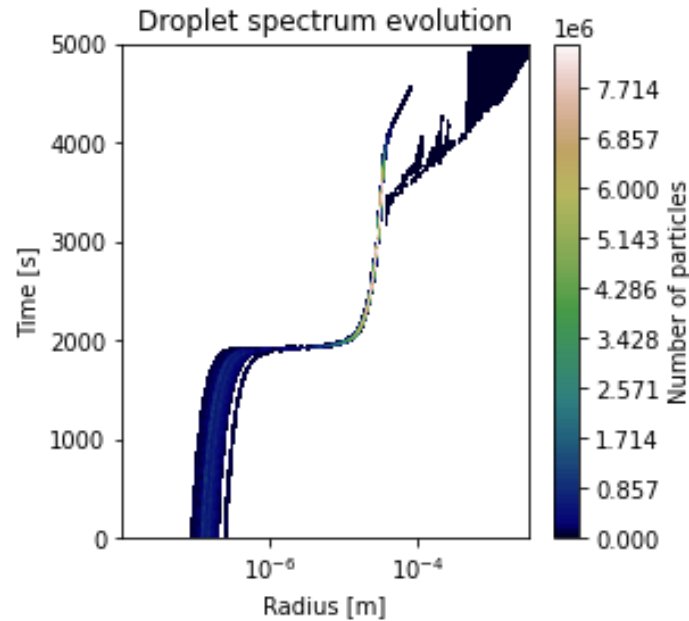


Figure 3.11 Spectra of cloud droplets for  $\sigma=1.2$

## Discussion

There are limitations to the numerical model used to answer the research question. First of all, the model does not take into account mixing during ascent. Mixing consists of interaction between one cloud parcel and the ones surrounding the same cloud parcel. This may affect the microphysical processes taking place in the parcel so that the output variables differ.

Secondly, the model doesn't consider droplets which fall to the ground without reaching the cloud top. This may have an influence on the cloud droplet number.

Furthermore, external forcing may have a significant influence on the microphysical processes. The model does not take into account this influence. Wind may influence the upward motion of the cloud parcel leading to changes in the parcel.

There is also a practical point of attention regarding marine cloud brightening using sea salt as aerosol. Sea salt may be abundantly available in oceans, it is dissolved. For marine cloud brightening, it can be only used as particles.

# Conclusions and Recommendations

## 5.1 Conclusions

The aerosol mean geometric radius at start, aerosol number concentration at start and the modal standard deviation of the initial aerosol spectrum of sea salt used for marine cloud brightening relate to the albedo of a brightened cloud as follows:

- The aerosol mean geometric radius at start does not affect the albedo of the brightened cloud.
- An increased aerosol number concentration at start leads to a higher albedo of the brightened cloud.
- An increased modal standard deviation of the initial aerosol spectrum, i.e. the variability in aerosol radius, leads to a lower albedo of the brightened cloud.

A higher initial aerosol number concentration results in a higher cloud droplet number leading to an increased cloud albedo. Furthermore, a smaller aerosol number concentration leads to a higher mean cloud droplet radius as the relative supersaturation is higher for smaller aerosol number concentrations. When the aerosol number concentration is constant, a changing aerosol mean geometric radius does neither lead to a change in albedo, nor to a change in mean cloud droplets radius.

A higher variability in aerosol radius at start leads to an uneven activation due to the occurrence of small aerosols and relatively bigger aerosols. The bigger aerosols tend to activate earlier than the smaller ones. Furthermore, through condensation their size increases making them collide and coalesce. When they get heavy enough, they precipitate. As a result, the cloud droplet number decreases. So does the cloud albedo.

## 5.2 Recommendations

For marine cloud brightening using sea salt aerosols, engineers are recommended to use an aerosol bulk composition with a limited variability in aerosol radius in order to achieve a higher albedo of the brightened cloud. Furthermore, it is recommended to spray a high number of sea salt aerosols for a higher albedo. The mean radius does not have an influence on the albedo and may be chosen based on other considerations.

For further research on cloud microphysics and modelling marine cloud brightening using aerosols, it is recommended to look at the use of other types of aerosol and their properties and make a comparison in order to find the best efficiency. Organic matter and algae, which are available in abundance in oceans like sea salt, can be considered. It is also recommended to look at other properties of sea salt as well, for example the roundness of the sea salt particles.

The model is based on a constant upward speed. It is recommended to consider forces on the aerosol parcel occurring due to external weather conditions like the wind.



# Appendix A

## Python code for plots aerosol mean geometric radius at start

```
# Importing packages
import numpy as np
import matplotlib.pyplot as plt
%matplotlib inline

# Change in mean radius while varying aerosol mean geometric radius at start (result1)
data15 = np.genfromtxt('result1_0.015.dat', delimiter = None, skip_header=3)
data20 = np.genfromtxt('result1_0.020.dat', delimiter = None, skip_header=3)
data45 = np.genfromtxt('result1_0.045.dat', delimiter = None, skip_header=3)
data85 = np.genfromtxt('result1_0.085.dat', delimiter = None, skip_header=3)
data170 = np.genfromtxt('result1_0.170.dat', delimiter = None, skip_header=3)
data200 = np.genfromtxt('result1_0.200.dat', delimiter = None, skip_header=3)

time = data45[:,0]
height = data45[:,1]
mr15 = data15[:,17] *10**6
mr20 = data20[:,17] *10**6
mr45 = data45[:,17] *10**6
mr85 = data85[:,17] *10**6
mr170 = data170[:,17] *10**6
mr200 = data200[:,17] *10**6

fig,a = plt.subplots(figsize=(8,10))
a.plot(mr15, time)
a.plot(mr20, time)
a.plot(mr45, time)
a.plot(mr85, time)
a.plot(mr170, time)
a.plot(mr200, time)

a.set_xlabel('Mean radius of cloud droplets ( $\mu\text{m}$ )', fontsize=14)
a.set_ylabel('Time (s)', fontsize=14)

a2 = a.twinx()
a2.plot(mr15, height)
a2.plot(mr20, height)
a2.plot(mr45, height)
a2.plot(mr85, height)
a2.plot(mr170, height)
a2.plot(mr200, height)

a2.set_ylabel('Height (m)', fontsize=14)

a.grid(linestyle='-')
a.set_title('Change in mean radius while varying aerosol mean geometric radius at start', color='black', fontsize=14)
a.legend(['rmg=0.015  $\mu\text{m}$ ', 'rmg=0.020  $\mu\text{m}$ ', 'rmg=0.045  $\mu\text{m}$ ', 'rmg=0.085  $\mu\text{m}$ ', 'rmg=0.170  $\mu\text{m}$ ', 'rmg=0.200  $\mu\text{m}$ '], fontsize=14,
         frameon=False)

# Change in Liquid number mixing ratio while varying aerosol mean geometric radius at start (result1)
time = data45[:,0]
height = data45[:,1]
lnmr15 = data15[:,13]
lnmr20 = data20[:,13]
lnmr45 = data45[:,13]
lnmr85 = data85[:,13]
lnmr170 = data170[:,13]
lnmr200 = data200[:,13]

fig,z = plt.subplots(figsize=(8,10))
z.plot(lnmr15, time)
z.plot(lnmr20, time)
z.plot(lnmr45, time)
z.plot(lnmr85, time)
z.plot(lnmr170, time)
z.plot(lnmr200, time)
```

```

z.set_xlabel('Liquid number mixing ratio (1/kg)', fontsize=14)
z.set_ylabel('Time (s)', fontsize=14)

z2 = z.twinx()
z2.plot(lnmr15, height)
z2.plot(lnmr20, height)
z2.plot(lnmr45, height)
z2.plot(lnmr85, height)
z2.plot(lnmr170, height)
z2.plot(lnmr200, height)

z2.set_ylabel('Height (m)', fontsize=14)

z.grid(linestyle='-')
z.set_title('Change in liquid number mixing ratio while varying aerosol mean geometric radius at start', color='black',
           fontsize=14)
z.legend(['rmg=0.015  $\mu\text{m}$ ', 'rmg=0.020  $\mu\text{m}$ ', 'rmg=0.045  $\mu\text{m}$ ', 'rmg=0.085  $\mu\text{m}$ ', 'rmg=0.170  $\mu\text{m}$ ', 'rmg=0.200  $\mu\text{m}$ '], fontsize=14,
         frameon=False)

# Change in relative supersaturation while varying aerosol mean geometric radius at start (result1)
time = data45[:,0]
height = data45[:,1]
rss15 = data15[:,6]
rss20 = data20[:,6]
rss45 = data45[:,6]
rss85 = data85[:,6]
rss170 = data170[:,6]
rss200 = data200[:,6]

fig,y = plt.subplots(figsize=(8,10))
y.plot(rss15, time)
y.plot(rss20, time)
y.plot(rss45, time)
y.plot(rss85, time)
y.plot(rss170, time)
y.plot(rss200, time)

y.set_xlabel('Relative supersaturation (-)', fontsize=14)
y.set_ylabel('Time (s)', fontsize=14)

y2 = y.twinx()
y2.plot(rss15, height)
y2.plot(rss20, height)
y2.plot(rss45, height)
y2.plot(rss85, height)
y2.plot(rss170, height)
y2.plot(rss200, height)

y2.set_ylabel('Height (m)', fontsize=14)

y.grid(linestyle='-')
y.set_title('Change in relative supersaturation while varying aerosol mean geometric radius at start', color='black',
           fontsize=14)
y.legend(['rmg=0.015  $\mu\text{m}$ ', 'rmg=0.020  $\mu\text{m}$ ', 'rmg=0.045  $\mu\text{m}$ ', 'rmg=0.085  $\mu\text{m}$ ', 'rmg=0.170  $\mu\text{m}$ ', 'rmg=0.200  $\mu\text{m}$ '], fontsize=14,
         frameon=False)
y.set_xlim(0,0.05)

# Change in albedo
rmg = np.array([0.015, 0.020, 0.045, 0.085, 0.170, 0.200])
albedos = np.array([0.86045611, 0.8614182, 0.86227529, 0.86238674, 0.86243485, 0.86245171])

fig,b = plt.subplots(figsize=(8,5))
b.plot(rmg,albedos,'rx',ms=10)
b.plot(rmg,albedos,'black',linewidth=1)
b.set_xlabel('Aerosol mean geometric radius at start ( $\mu\text{m}$ )', fontsize=14)
b.set_ylabel('Albedo (-)', fontsize=14)
b.set_ylim(0.65,0.92)
b.grid(linestyle='-')
b.set_title('Change in albedo', fontsize=14);

```

# Appendix B

## Python code for plots aerosol number concentration at start

```
# Change in mean radius while varying aerosol number concentration at start (result2)
data5 = np.genfromtxt('result2_5.dat', delimiter = None, skip_header=3)
data10 = np.genfromtxt('result2_10.dat', delimiter = None, skip_header=3)
data15 = np.genfromtxt('result2_15.dat', delimiter = None, skip_header=3)
data20 = np.genfromtxt('result2_20.dat', delimiter = None, skip_header=3)
data25 = np.genfromtxt('result2_25.dat', delimiter = None, skip_header=3)
data30 = np.genfromtxt('result2_30.dat', delimiter = None, skip_header=3)

height = data5[:,1]
time = data5[:,0]

mr5 = data5[:,17] *10**6
mr10 = data10[:,17] *10**6
mr15 = data15[:,17] *10**6
mr20 = data20[:,17] *10**6
mr25 = data25[:,17] *10**6
mr30 = data30[:,17] *10**6

lnmr5 = data5[:,13]
lnmr10 = data10[:,13]
lnmr15 = data15[:,13]
lnmr20 = data20[:,13]
lnmr25 = data25[:,13]
lnmr30 = data30[:,13]

rss5 = data5[:,6]
rss10 = data10[:,6]
rss15 = data15[:,6]
rss20 = data20[:,6]
rss25 = data25[:,6]
rss30 = data30[:,6]

fig,c = plt.subplots(figsize=(8,10))
c.plot(mr5,time)
c.plot(mr10,time)
c.plot(mr15,time)
c.plot(mr20,time)
c.plot(mr25,time)
c.plot(mr30,time)

c.set_xlabel('Mean radius of cloud droplets ( $\mu\text{m}$ )', fontsize=14)
c.set_ylabel('Time (s)', fontsize=14)

c2=c.twinx()
c2.plot(mr5,height)
c2.plot(mr10,height)
c2.plot(mr15,height)
c2.plot(mr20,height)
c2.plot(mr25,height)
c2.plot(mr30,height)

c2.set_ylabel('Height (m)', fontsize=14)

c.grid(linestyle='-')
c.set_title('Change in mean radius while varying aerosol number concentration at start', fontsize=14)
c.legend(['N=5e6/m3', 'N=10e6/m3', 'N=15e6/m3', 'N=20e6/m3', 'N=25e6/m3', 'N=30e6/m3'], fontsize=14, frameon=False)

# Change in liquid number mixing ratio while varying aerosol number concentration at start (result2)
fig,d = plt.subplots(figsize=(8,10))
d.plot(lnmr5,time)
d.plot(lnmr10,time)
d.plot(lnmr15,time)
d.plot(lnmr20,time)
d.plot(lnmr25,time)
d.plot(lnmr30,time)
```

```

d.set_xlabel('Liquid number mixing ratio (1/kg)', fontsize=14)
d.set_ylabel('Time (s)', fontsize=14)

d2=d.twinx()
d2.plot(lnmr5,height)
d2.plot(lnmr10,height)
d2.plot(lnmr15,height)
d2.plot(lnmr20,height)
d2.plot(lnmr25,height)
d2.plot(lnmr30,height)

d2.set_ylabel('Height (m)', fontsize=14)

d.grid(linestyle='-')
d.set_title('Change in liquid number mixing ratio while varying aerosol number concentration at start',fontsize=14)
d.legend(['N=5e6/m3', 'N=10e6/m3', 'N=15e6/m3', 'N=20e6/m3', 'N=25e6/m3', 'N=30e6/m3'], fontsize=14, frameon=False)

# Change in relative supersaturation while varying aerosol number concentration at start (result2)
fig,w = plt.subplots(figsize=(8,10))
w.plot(rss5,time)
w.plot(rss10,time)
w.plot(rss15,time)
w.plot(rss20,time)
w.plot(rss25,time)
w.plot(rss30,time)

w.set_xlabel('Relative supersaturation (-)', fontsize=14)
w.set_ylabel('Time (s)', fontsize=14)

w2=w.twinx()
w2.plot(rss5,height)
w2.plot(rss10,height)
w2.plot(rss15,height)
w2.plot(rss20,height)
w2.plot(rss25,height)
w2.plot(rss30,height)

w2.set_ylabel('Height (m)', fontsize=14)

w.grid(linestyle='-')
w.set_title('Change in relative supersaturation while varying aerosol number concentration at start', fontsize=14)
w.legend(['N=5e6/m3', 'N=10e6/m3', 'N=15e6/m3', 'N=20e6/m3', 'N=25e6/m3', 'N=30e6/m3'], fontsize=14, frameon=False)
w.set_xlim(0,0.015)

# Change in albedo
N = np.arange(5,31,5)
albedos = np.array([0.83188086, 0.86238674, 0.87780154, 0.88786807, 0.89509742, 0.90075006])

fig,e = plt.subplots(figsize=(8,5))
e.plot(N,albedos,'rx', ms=10)
e.plot(N,albedos,'black',linewidth=1)
e.set_ylabel('Albedo (-)', fontsize=14)
e.set_xlabel('Aerosol number concentration at start (1/m3), x 10e6', fontsize=14)

e.set_ylim(0.65,0.92)
e.set_title('Change in albedo', fontsize=14)
e.grid(linestyle='-')

```

# Appendix C

## Python code for plots modal standard deviation of initial aerosol spectrum

```
# Change in mean radius while varying standard deviation of initial aerosol spectrum
run10 = np.genfromtxt('result3_10.dat', delimiter = None, skip_header=3)
run12 = np.genfromtxt('result3_12.dat', delimiter = None, skip_header=3)
run14 = np.genfromtxt('result3_14.dat', delimiter = None, skip_header=3)
run16 = np.genfromtxt('result3_16.dat', delimiter = None, skip_header=3)
run18 = np.genfromtxt('result3_18.dat', delimiter = None, skip_header=3)
run20 = np.genfromtxt('result3_20.dat', delimiter = None, skip_header=3)

time = run10[:,0]
height = run10[:,1]

mr10 = run10[:,17] *10**6
mr12 = run12[:,17] *10**6
mr14 = run14[:,17] *10**6
mr16 = run16[:,17] *10**6
mr18 = run18[:,17] *10**6
mr20 = run20[:,17] *10**6

fig,f = plt.subplots(figsize=(8,10))
f.plot(mr10,time)
f.plot(mr12,time)
f.plot(mr14,time)
f.plot(mr16,time)
f.plot(mr18,time)
f.plot(mr20,time)

f.set_ylabel('Time (s)', fontsize=14)
f.set_xlabel('Mean radius of cloud droplets ( $\mu\text{m}$ )', fontsize=14)

f2 = f.twinx()
f2.plot(mr10,height)
f2.plot(mr12,height)
f2.plot(mr14,height)
f2.plot(mr16,height)
f2.plot(mr18,height)
f2.plot(mr20,height)

f2.set_ylabel('Height (m)', fontsize=14)

f.grid(linestyle='-')
f.set_title('Change in mean radius while varying standard deviation of initial aerosol spectrum',fontsize=14)
f.legend([' $\sigma=1.0$ ', ' $\sigma=1.2$ ', ' $\sigma=1.4$ ', ' $\sigma=1.6$ ', ' $\sigma=1.8$ ', ' $\sigma=2.0$ '], fontsize=14, frameon=False)
```

```
# Change in liquid number mixing ratio while varying standard deviation of initial aerosol spectrum
lr10 = run10[:,13]
lr12 = run12[:,13]
lr14 = run14[:,13]
lr16 = run16[:,13]
lr18 = run18[:,13]
lr20 = run20[:,13]

fig,h = plt.subplots(figsize=(8,10))
h.plot(lr10,time)
h.plot(lr12,time)
h.plot(lr14,time)
h.plot(lr16,time)
h.plot(lr18,time)
h.plot(lr20,time)

h.set_xlabel('Liquid number mixing ratio (1/kg)', fontsize=14)
h.set_ylabel('Time (s)', fontsize=14)
```

```

h2 = h.twinx()
h2.plot(lr10,height)
h2.plot(lr12,height)
h2.plot(lr14,height)
h2.plot(lr16,height)
h2.plot(lr18,height)
h2.plot(lr20,height)

h2.set_ylabel('Height (m)', fontsize=14)

h.grid(linestyle='-')
h.set_title('Change in liquid number mixing ratio while varying standard deviation of initial aerosol spectrum',fontsize=14)
h.legend([' $\sigma=1.0$ ', ' $\sigma=1.2$ ', ' $\sigma=1.4$ ', ' $\sigma=1.6$ ', ' $\sigma=1.8$ ', ' $\sigma=2.0$ '], fontsize=14, frameon=False)

# Change in relative supersaturation while varying standard deviation of initial aerosol spectrum
rs10 = run10[:,6]
rs12 = run12[:,6]
rs14 = run14[:,6]
rs16 = run16[:,6]
rs18 = run18[:,6]
rs20 = run20[:,6]

fig,v = plt.subplots(figsize=(8,10))
v.plot(rs10,time)
v.plot(rs12,time)
v.plot(rs14,time)
v.plot(rs16,time)
v.plot(rs18,time)
v.plot(rs20,time)

v.set_xlabel('Relative supersaturation (-)', fontsize=14)
v.set_ylabel('Time (s)', fontsize=14)

v2 = v.twinx()
v2.plot(rs10,height)
v2.plot(rs12,height)
v2.plot(rs14,height)
v2.plot(rs16,height)
v2.plot(rs18,height)
v2.plot(rs20,height)

```

```

v2.set_ylabel('Height (m)', fontsize=14)

v.grid(linestyle='-')
v.set_title('Change in relative supersaturation while varying standard deviation of initial aerosol spectrum',fontsize=14)
v.legend([' $\sigma=1.0$ ', ' $\sigma=1.2$ ', ' $\sigma=1.4$ ', ' $\sigma=1.6$ ', ' $\sigma=1.8$ ', ' $\sigma=2.0$ '], fontsize=14, frameon=False)

#v.set_xlim(0.012,0.013)
#v2.set_ylim(595,605)

# Change in albedo
sigma = np.arange(1,2.1,0.2)
alb = ([0.86238674, 0.75549278, 0.75116741, 0.72390403, 0.7052053, 0.69129736])

fig,g = plt.subplots(figsize=(8,5))
g.plot(sigma,alb,'rx',ms=10)
g.plot(sigma,alb,'black', linewidth=1)
g.set_xlabel('standard deviation of initial aerosol spectrum (-)', fontsize=14)
g.set_ylabel('Albedo (-)', fontsize=14)

g.set_title('Change in albedo', fontsize=14)
g.set_ylim(0.65,0.90)
g.grid(linestyle='-')

```

# References

- Boers, R., Mitchell, R.M. (1994). Absorption feedback in stratocumulus clouds Influence on cloud top albedo. *Tellus A: Dynamic Meteorology and Oceanography*, 46:3, 229-241, DOI: 10.3402/tellusa.v46i3.15476
- Connolly, P. J., McFiggans, G. B., Wood, R., & Tsiamis, A. (2014). Factors determining the most efficient spray distribution for marine cloud brightening. *Philosophical Transactions of the Royal Society*. A372:2040056. <https://doi.org/10.1098/rsta.2014.0056>
- Gadian, A. (2009). *Whitening the clouds*. National Environment Research Council. <https://nerc.ukri.org/planetearth/stories/584/>
- Glassmeier, F. (2020). *Introduction to the adiabatic cloud parcel model*. Wageningen University.
- Guelle, W., Schulz, M., Balkanski, Y., & Dentener, F. (2001). Influence of the source formulation on modeling the atmospheric global distribution of sea salt aerosol. *Journal of Geophysical Research Atmospheres*, 106 (D21), 27509–27524. <https://doi.org/10.1029/2001JD900249>
- Horowitz, H. M., Holmes, C., Wright, A., Sherwen, T., Wang, X., Evans, M., Huang, J., Jaeglé, L., Chen, Q., Zhai, S., & Alexander, B. (2020). Effects of Sea Salt Aerosol Emissions for Marine Cloud Brightening on Atmospheric Chemistry: Implications for Radiative Forcing. *Geophysical Research Letters*, 47, e2019GL085838. <https://doi.org/10.1029/2019GL085838>
- IPCC (2017). *About the IPCC*. Retrieved October 17, 2020, from <https://www.ipcc.ch/about/>
- IPCC (2014). *Climate Change 2014 Synthesis Report Summary for Policymakers Summary for Policymakers* (Fifth Assessment Report).
- Latham, J., Bower, K., Choullarton, T., Coe, H., Connolly, P., Cooper, G., Craft, T., Foster, J., Gadian, A., Galbraith, L., Iacovides, H., Johnston, D., Launder, B., Leslie, B., Meyer, J., Neukermans, A., Ormond, B., Parkes, B., Rasch, P., ..., Wood, R. (2012). Marine cloud brightening. *Philosophical Transactions of the Royal Society A: Mathematical, Physical and Engineering Sciences*, 370 (1974), 4217–4262. <https://doi.org/10.1098/rsta.2012.0086>
- Met Office (2020). *Stratocumulus Clouds*. Retrieved October 21, 2020, from <https://www.metoffice.gov.uk/weather/learn-about/weather/types-of-weather/clouds/low-level-clouds/stratocumulus>
- National Library of Medicine (2020). *Sodium Chloride*. Retrieved October 21, 2020, from <https://pubchem.ncbi.nlm.nih.gov/compound/Sodium-chloride>
- Poloczanska, E. S., Burrows, M. T., Brown, C. J., Molinos, J. G., Halpern, B. S., Hoegh-Guldberg, O., Kappel, C. v., Moore, P. J., Richardson, A. J., Schoeman, D. S., & Sydeman, W. J. (2016). Responses of marine organisms to climate change across oceans. *Frontiers in Marine Science*. 3:62. 1–21. <https://doi.org/10.3389/fmars.2016.00062>
- Rahmstorf, S. (2007). A Semi-Empirical Approach to Projecting Future Sea-Level Rise. *Science*, 315 (5810), 368–371.